Frequency Multiplexing and Waveform Synthesis in Joint Communications and Sensing

Husheng Li

***Abstract*—The technique of joint communications and sensing (JCS) integrates both functions in the same waveform, thus reusing the frequency spectrum, transmit power and hardware. The two functions need to be multiplexed, while they also benefit each other. In this paper, the function multiplexing of JCS is in the frequency domain, leveraging the orthogonal subcarriers in orthogonal frequency division multiplexing (OFDM). To exploit the mutual benefits of subcarriers dedicated to communications and sensing, the signals over the communication subcarriers are leveraged for the function of sensing. The signals over the dedicated sensing subcarriers are made adaptive to the communication signals, in order to optimize the integrated sidelobe levels (ISLs) of the overall waveform and improve the sensing performance. Since the signals over the dedicated sensing subcarriers are functions of the communication signals, due to the adaptive waveform synthesis, they provide redundancies for the communication signals and improve the reliability of data transmission. The proposed JCS scheme is demonstrated by numerical results.**

I. Introduction

As a potential and promising technology in 6G communication systems, joint communications and sensing (JCS) are expected to substantially improve the efficiency of frequency spectrum, transmit power and hardware cost [1]–[5]. In JCS, the transceiver emits electromagnetic (EM) wave, which is modulated by communication data. The EM wave reaches the communication receiver and delivers the data, thus accomplishing the task of communication. Meanwhile, when the EM wave is reflected by a target (possibly the communication receiver itself), the reflected EM wave propagates back to the JCS transceiver, which is used for inferring the information of the target, thus accomplishing the task of sensing. Since both functions of communications and sensing are completed in the same round of EM wave propagation, the same frequency spectrum, transmit power and hardware are shared by both functions, thus being expected to achieve higher efficiency.

A major challenge in JCS is the waveform synthesis which needs to consider both functions. One can consider the waveform synthesis as the multiplexing of two functions, similarly to the multiplexing of data traffics to different destinations in communication networks. Therefore, the multiplexing could be orthogonal in the time, frequency or space[1], or non-orthogonally superimposed with mutual interference[2].

H. Li is with the Department of Electrical Engineering and Computer Science, the University of Tennessee, Knoxville, TN (email: husheng@eecs.utk.edu, phone number: 865-974-3861, address: 312 Min Kao Building, 1520 Middle Drive, Knoxville, TN, 37996).

[1]In communication systems, these approaches correspond to TDM, FDM and SDM, respectively.

[2]In communication systems, this corresponds to CDM or more advanced approaches such as dirty paper coding.

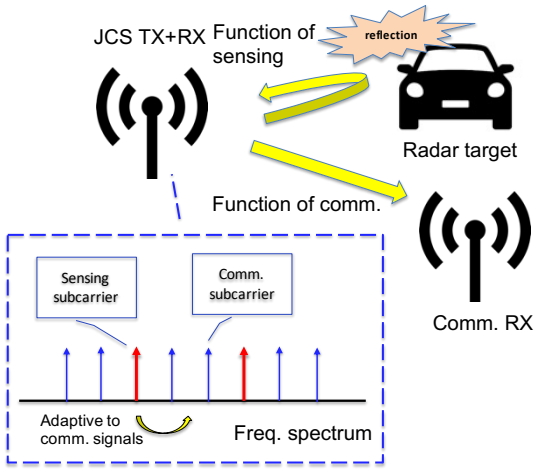

Fig. 1: JCS with function multiplexing

However, different from pure data communications, in which different data traffics are independent of each other, in JCS the communication and sensing functions are beneficial to each other. For example, the communication signal can also be used for sensing: (a) it provides bandwidth and power for sensing; (b) its pseudo-random time-domain sequence provides timing for ranging; (c) the data modulation facilitates the pulse compression in radar sensing.

In this paper, we consider multiplexing the functions of communications and sensing orthogonally in the frequency domain, using the orthogonal frequency division multiplexing (OFDM) signaling, which is popular in both data communications and radar sensing. In particular, we consider the interleaving structure of subcarriers dedicated to communications and sensing, respectively, as illustrated in Fig. 1. All the signals over all subcarriers, including the communication ones, will be used for sensing. The signals over the dedicated sensing subcarriers are synthesized adaptively to the signals over the communication subcarriers that are determined by the random data, in order to optimize the ambiguity function (AF) of the waveform. Since the signals over the sensing subcarriers are determined by the communication signals, they can be used as redundancies of the communication data, similarly to parity check bits in error correction codes, in order to provide extra protections for the data communications. Then, the major challenges of the design include (a) how to synthesize the signals over the dedicated sensing subcarriers for improving the sensing performance? (b) how to leverage the redundancy incurred by the adaptive sensing signals for enhancing the data communication reliability?

The remainder of this paper is organized as follows. Existing researches related to this paper are briefed in Section II. The system model is introduced in Section III. Then, the adaptive waveform synthesis, in order to optimize the sensing performance, is discussed in Section IV. As the benefit of sensing signals for communications, the error correction coding using sensing signals for protecting the communication data is studied in Section V. Numerical results are given in Section VI, while the conclusions are drawn in Section VII.

II. Related Works

In this section, we introduce existing studies related to this paper.

A. JCS: State of the Art

For the technique of JCS, comprehensive surveys can be found in [2]–[6]. Theoretical studies on the performance bounds of co-existing communications and sensing can be found in [7]–[12]. With multiple antennas, the spatial separation of the two functions via beamforming [2], [4], [5] achieves higher spectral efficiency than the time/frequency separation. Typical radar waveforms, particularly the frequency modulation continuous waveform (FMCW) and stepped frequency waveforms, have been leveraged to convey embedded information [13]–[16]. However, these studies did not fully exploit the mutual benefit between the functions of communications and sensing.

B. Radar Waveform Synthesis

The radar waveform can be synthesized either analytically or numerically. Different codes such as Golomb codes or Zadoff-Chu codes [17] have been proposed. Various optimization algorithms for waveform synthesis are summarized in [18]. These approaches are mainly focused on the minimization of sidelobes, which will also be used in this paper. An alternative criterion is to reduce the peak-average-power ratio (PAPR), for OFDM communications [19] and multi-carrier radar sensing [17]. The corresponding approaches include the waveform clipping [20], balancing [21], and peak reduction subcarriers [22], et al. This paper will adopt an approach similar to the peak reduction subcarriers [22].

III. System Model

In this section, we introduce the system model of JCS.

A. Signaling Scheme

We consider OFDM signaling with M subcarriers, where M is an even number. The beginning frequency is f_c and the frequency spacing is δf. The transmitted signal is given by

$$x(t) = \sum_{m=0}^{M-1} X_m e^{j(2\pi(f_c+m\delta_f)t+\phi_m)},\ t \in [0, T_p], \tag{1}$$

where T_p is the OFDM symbol duration equaling $\frac{1}{\delta f}$, X_m is the signal over the m-th subcarrier, which is a quadratic amplitude modulation (QAM) symbol if it is allocated for communications, or a complex-valued signal used for sensing, and ϕ_m is the corresponding phase.

The sets of subcarriers dedicated to communications and sensing are denoted by $\mathcal{S}_c$ and $\mathcal{S}_s$, respectively. One special case that will be discussed later is

$$\begin{cases} \mathcal{S}_c = \{1, 3, ..., 2M-1\} \\ \mathcal{S}_s = \{2, 4, ..., 2M\} \end{cases}, \tag{2}$$

namely half of the subcarriers are dedicated to communications (sensing).

B. Performance Metrics

Due to the dual functions in JCS, we need to consider the performance metrics of communications and sensing.

1) Sensing: The performance of sensing is usually featured by the AF of the waveform [18], which characterizes the resolution of radar sensing in the range-Doppler plane. For a generic signal x, the corresponding AF is defined as

$$\chi(\tau, f) = \int_{-\infty}^{\infty} x(t)x^*(t-\tau)e^{-j2\pi f(t-\tau)}dt, \tag{3}$$

where τ is time delay and f is the frequency offset. When f is set to 0, the AF becomes the time-domain autocorrelation r for assessing the ranging peformance, namely

$$r(\tau) \quad = \quad \int_{\tau}^{T_p} x(t)x^*(t-\tau)dt. \tag{4}$$

When τ is set to 0, the AF becomes the Doppler-domain Fourier transform characterizing the velocity estimation performance, namely

$$D(f) \quad = \quad \int_{\tau}^{T_p} |x(t)|^2 e^{-j2\pi ft}dt. \tag{5}$$

For simplicity of analysis, we consider only the AF along the τ-axis and the f-axis. For assessing the τ-section of AF that features the performance of ranging, we sample the autocorrelation function and obtain $r[k] = r(kT_c)$, where $T_c = \frac{T_p}{M}$ is the chip period[3]. We use the integrated sidelobe level (ISL) [18] to characterize the radar sensing performance:

$$\xi_r = \sum_{k=-(M-1),k\neq 0}^{M-1} |r[k]|^2 = 2\sum_{k=1}^{M-1} |r[k]|^2, \tag{6}$$

where $M-1$ sidelobes are taken into account and the subscript r means ranging. A smaller ISL is desired, since it indicates less self-interference from the sidelobes and higher resolution of target identification. Similarly to the ISL of ranging, we can also sample the Doppler spectrum $D(f)$ and calculate the ISL, namely

$$\xi_d = \sum_{k=-(M-1),k\neq 0}^{M-1} |D[k]|^2 = 2\sum_{k=1}^{M-1} |D[k]|^2, \tag{7}$$

where $D[k] = D(k\delta f)$ and the subscript d means the ISL for Doppler. Similarly, we also desire a smaller value of ξ_d. We call the above definitions of ISLs the ranging ISL (R-ISL) and Doppler ISL (D-ISL).

[3]The M chips are the IDFT of the M symbols on the M subcarriers.

2) Communications: The metric for communications is much more straightforward. We use the symbol error rate over each subcarrier to measure the reliability of data transmission, which also determines the overall channel capacity if coding is carried out across different subcarriers.

IV. Adaptive Waveform Synthesis

In this section, we study the synthesis of the signals over the dedicated sensing subcarriers $\mathcal{S}_s$. Note that the signals over the communication subcarriers are generated from the communication data, in the same manner as in pure communication systems. Then, the dedicated sensing signals are synthesized adaptively to the instantaneous communication data, thus being also random to the communication receiver.

A. Power Allocation for Ranging

We approximate the samples of the autocorrelation by the circular autocorrelation of the sampled signal, which is given by

$$r[k] \approx \sum_{n=0}^{M} x[n]x^*[\text{mod}(n-k, M)], \tag{8}$$

where $x[n] = x(nT_c)$. The reason for the circular autocorrelation is for the simplicity of analysis; meanwhile, the prefix of each OFDM symbol is also taken into the calculation of autocorrelation, thus achieving a partial circular correlation. Then, the R-ISL is given by the frequency-domain power spectral density (PSD) $\{|X_k|^2\}_{k=0,\ldots,M-1}$ using the following Parseval equality:

$$\sum_{k=0}^{M-1} r^2[k] = \frac{1}{M}\sum_{k=0}^{M-1} |X_k|^4, \tag{9}$$

which results in the analytic expression of ξ_R:

$$\begin{aligned}
\xi_R &= 2\sum_{k=1}^{M-1} r^2[k] \\
&= 2\left(\sum_{k=0}^{M-1} r^2[k] - r^2[0]\right) \\
&= 2\left(\frac{1}{M}\sum_{k=0}^{M-1} |X_k|^4 - \left(\frac{1}{M}\sum_{k=0}^{M-1} |X_k|^2\right)^2\right) \\
&= 2Var(\{|X_k|^2\}_{k=0,\ldots,M-1}),
\end{aligned} \tag{10}$$

where the third equality leverages (8) and the Parseval equality $r^2[0] = \frac{1}{M}\sum_{k=0}^{M-1}|X_k|^2$, and Var is the variance.

From (10), we observe that the R-ISL depends on only the power of the subcarriers; more precisely, it is the variance of the PSD of the spectrum. Therefore, for minimizing the R-ISL, we simply allocate equal powers to the subcarriers dedicated to sensing.

B. Phase Allocation for Doppler

When the powers of the sensing subcarriers are allocated, we adjust the corresponding phases for optimizing the D-ISL ξ_d. From (7), we observe that the D-ISL represents the non-DC components of the Fourier transform of the time-domain power profile $\{|x(t)|^2\}_t$. When the time-domain signal has a constant envelop, the D-ISL ξ_d is nullified, thus achieving a perfect performance in the AF for the purpose of Doppler estimation. To making the time-domain power profile more constant, an intuitive approach is to reduce the PAPR in the time-domain waveform, which has been intensively studied in the context of OFDM communications [19] and multi-carrier radar sensing [17].

There have been substantial studies on the PAPR reduction since the deployment of OFDM-based LTE networks. One effective approach is to use iterative gradient descent to refine the flexible signals over the sensing subcarriers (see Section 8.10 (Peak Reduction Carriers) in [19]). However, as explained in the introduction, we expect the signals over the sensing subcarriers to provide redundancy (thus error detection or correction) for the communications. When iterative gradient descent is utilized, the mapping from the communication symbols to the sensing signals is highly complex, thus making it difficult to leverage the corresponding redundancy during the decoding procedure at the communication receiver.

Therefore, in this paper, we propose a simple approach to handle the PAPR with a simple mapping from the communication signals to the sensing signals. We consider the subcarrier assignment in (2), namely the odd (even) subcarriers are used for communications (sensing). For notational simplicity, we consider QPSK modulation in the communication subcarriers.

For simplicity, we consider only the real part is calculated, while the imaginary part can be processed similarly. The signal amplitudes of the communication and sensing subcarriers are assumed to be identical, which will be relaxed later. Now, considering the pair of subcarriers $2m$ and $2m-1$, we calculate the sum of their signals:

$$\begin{aligned}
& \cos(2\pi(f_0 + 2m\delta f)t + \theta_{2m}) \\
+\ & \cos(2\pi(f_0 + (2m-1)\delta f)t + \theta_{2m-1}) \\
=\ & 2\cos\left(2\pi(f_0 + \frac{1}{2}(4m-1)\delta f)t + \frac{1}{2}(\theta_{2m} + \theta_{2m-1})\right) \\
\times\ & \cos\left(\pi\delta f t + \frac{1}{2}(\theta_{2m} - \theta_{2m-1})\right),
\end{aligned} \tag{11}$$

where the sum is an amplitude modulation (AM) signal with carrier frequency $f_0 + \frac{1}{2}(4m-1)$ and slowly changing envelop $\cos\left(\pi\delta f t + \frac{1}{2}(\theta_{2m} - \theta_{2m-1})\right)$.

Therefore, we can consider the waveform as the sum of $M/2$ AM signals having different effective carrier frequencies $\left\{f_0 + \frac{1}{2}(4m-1)\delta f\right\}_{m=1,\ldots,M}$ and slowly changing modulating signals. We assume that, when the effective carrier frequencies are large, the envelop of the overall waveform can be approximated by the sum of the individual envelops, namely

$$E(t) \approx \sum_{k=1}^{M/2} \cos\left(\pi\delta f t + \frac{1}{2}(\theta_{2m} - \theta_{2m+1})\right), \tag{12}$$

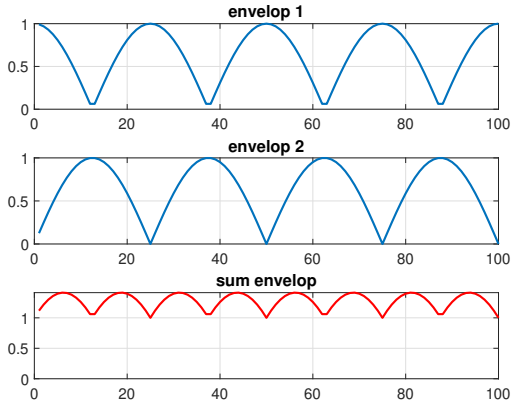

Fig. 2: Sum of cosine envelops

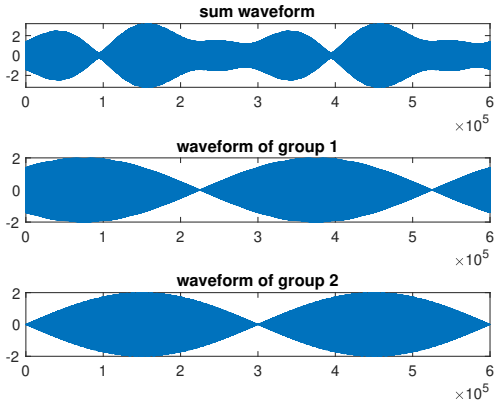

Fig. 3: Envelops of phase-calibrated subcarrier pairs

To make the envelop close to a constant, we set

$$\frac{1}{2}\left(\theta_{2m}-\theta_{2m-1}\right)=\frac{\pi}{M}, \tag{13}$$

namely the phase of the sensing signal over subcarrier $2m$ is set to be

$$\theta_{2m}=\theta_{2m-1}+\frac{2\pi}{M}. \tag{14}$$

Take $M=4$ for instance. The four subcarriers form two AM signals with phase difference $\frac{\pi}{2}$. The envelops of the two AM signals and the sum are shown in Fig. 2. We can observe that the sum of the envelop is time-varying but still has small variations. The synthesized time-domain waveform is shown in Fig. 3, together with which the two AM signals are shown. We observe that the simulated waveform in Fig. 3 has significantly more variations in the expected one in Fig. 2. The reason is that the approximation in (12), because the carrier frequencies $f_c+\frac{1}{2}\delta f$ and $f_c+\frac{5}{2}\delta f$ has a frequency difference $2\delta f$, thus resulting in a beat of frequency $2\delta f$ and the amplitude fades. However, compared with the envelop for random phase difference between the AM signals (shown in Fig. 4), the waveform of the proposed scheme is still more uniform, thus resulting in a better Doppler spectrum. More details with more subcarriers will be given in the section of numerical simulations.

In the above analysis, we assume that all subcarriers have the same power and use QPSK. When the amplitudes of the communication and sensing signals are different, we can still adjust the phase of the sensing subcarrier, namely rewriting

$$\begin{aligned} & A_{2m}\cos(2\pi(f_0+2m\delta f)t+\theta_{2m}) \\ + \;& A_{2m-1}\cos(2\pi(f_0+(2m-1)\delta f)t+\theta_{2m-1}) \\ = \;& \tilde{A}_m(t)\cos\left(\pi(4m-1)\delta f t+\frac{\theta_{2m}+\theta_{2m-1}}{2}+\phi(t)\right), \end{aligned} \tag{15}$$

where the time-varying amplitude $\tilde{A}_m(t)$ is given by

$$\tilde{A}_m(t)=\sqrt{A_{2m}^2+A_{2m-1}^2+A_{2m}A_{2m-1}\psi(t)}, \tag{16}$$

where $\psi(t)$ is given by

$$\psi(t)=\cos(2\pi\delta f t+(\theta_{2m}-\theta_{2m-1})), \tag{17}$$

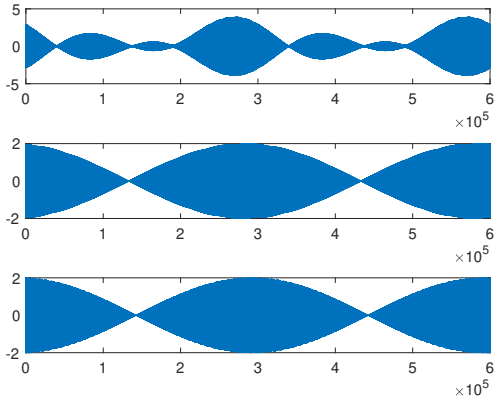

Fig. 4: Envelops of random phase subcarrier pairs

and the phase ϕ is given by

$$\phi(t)=\frac{A_{2m}-A_{2m-1}}{A_{2m}+A_{2m-1}}\tan\left(\pi\delta f t+\frac{\phi_{2m}-\phi_{2m-1}}{2}\right). \tag{18}$$

Again, we can see that the sum of the two signals is still the product of a slowly changing amplitude and a high-frequency oscillation. Due to the square root in (16), when $A_{2m}\approx A_{2m-1}$, $\tilde{A}_m(t)$ is close to a cosine function with phase difference $\frac{\theta_{2m}-\theta_{2m-1}}{2}$ and justifies the phase setup in (14). When $A_{2m}\gg A_{2m+1}$ (or vice versa), we have

$$\tilde{A}_m(t)\approx A_{2m}+2A_{2m-1}\psi(t), \tag{19}$$

at which it is desirable to set

$$\theta_{2m}=\theta_{2m-1}+\frac{\pi}{M}. \tag{20}$$

It is our future work to address the intermediate case of A_{2m} and A_{2m-1}.

V. Sensing Signal for Redundancy

In this section, we study how to use the signals over the dedicated sensing subcarriers as the redundancy of communication signals, in order to improve the reliability of data transmission. This benefit is based on the proposed sensing scheme in which the sensing signals are used to refine the

overall waveform for the purpose of sensing, and are thus deterministic functions of the communication signals.

For simplicity, we assume QPSK modulation and consider the following a posterior probability:

$$\begin{aligned} P(\theta_{2m}|\mathbf{r}) &\propto P(\mathbf{r}|\theta_{2m}) \\ &= P(r_{2m}, r_{2m-1}|\theta_{2m}) \\ &= P(r_{2m}|\theta_{2m}(\theta_{2m-1}))P(r_{2m-1}|\theta_{2m-1}), \quad (21) \end{aligned}$$

where $\mathbf{r}$ is the received signal, and the phase θ_{2m} on the $2m$-th subcarrier is a function of θ_{2m-1}, due to the scheme of waveform synthesis in the last section. We use the maximum a posterior (MAP) criterion for the demodulation:

$$\theta_{2m-1} = \arg\max_{\theta} P(r_{2m}|\theta_{2m}(\theta))P(r_{2m-1}|\theta), \qquad (22)$$

where the condition probability $P(r|\theta)$ is based on the probabilistic distribution of signal conditioned on the phase. It can be easily implemented by exhaustive search over the constellation of QAM. The demodulation can be extended to generic case of QAM straightforwardly.

VI. Numerical Results

In this section, we provide numerical results to demonstrate the proposed JCS algorithms. Throughout the simulations, we fix the initial carrier frequency is 2.5GHz and the frequency space $\delta f = 120$kHz.

A. Ranging ISL

We first tested the performance of R-ISL. In Fig. 5, we plotted the R-ISL (normalized by $r^2[0]$) for random QAM symbols (all subcarriers dedicated to communications) and calibrated sensing carriers (in which all sensing subcarriers are allocated the same power in order to reduce the variance of powers over different subcarriers and the phases are set as in (14)). The R-ISL is plotted versus different numbers of subcarriers with fixed 64-QAM modulation. We observe that the dedicated sensing subcarriers substantially reduce the R-ISL, thus significantly improving the sensing resolution. We also notice that the R-ISL almost does not change for different numbers of subcarriers.

The R-ISL versus different orders of QAM (ranging from 4 to 1024) is plotted in Fig. 6, when the number of subcarriers is fixed at 512. Again, we observe the substantial performance gain of the proposed power allocation. An alternative interesting observation is that the R-ISL increases with the order of QAM (thus more irregularity in the power) and saturates when the order of QMA is above 128.

B. Doppler ISL

The cumulative distribution functions (CDFs) of PAPR and D-ISL are plotted in Fig. 7, when the number of subcarriers is 4. We observe that both are substantially reduced by the proposed phase difference in (14). The corresponding CDFs are plotted for the case of 64 subcarriers. We observe that the performance gain is significantly reduced. In our further simulations, when $M > 128$, the performance gain becomes marginal. Therefore, the proposed phase difference calibration

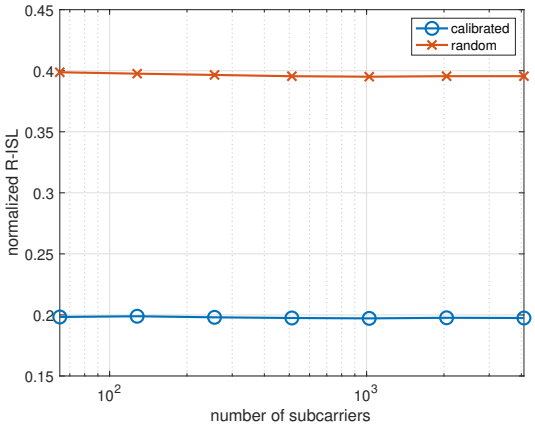

Fig. 5: Comparison of R-ISL between random phase and calibrated phase for different numbers of subcarriers.

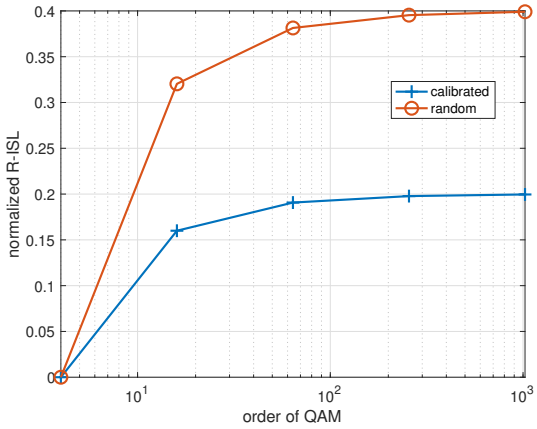

Fig. 6: Comparison of ranging ISL between random phase and calibrated phase for different orders of QAM.

is valid for only small number of subcarriers. For more subcarriers, the beat frequency due to the frequency difference in the AM signals causes more random power oscillations, thus making the performance gain vanish.

C. Communication Performance

The symbol error rates (SER), with or without the assistance from sensing subcarriers, are plotted in Fig. 9. The order of QAM is fixed at 64. The SNR ranges from -10dB to 25dB. We observe that the SER is substantially reduced by incorporating the redundancy provided by the sensing subcarriers.

VII. Conclusions

The function multiplexing in JCS has been studied, in which the mutual benefits between the two functions have been analyzed. The subcarriers of OFDM signaling are divided into subsets of communication and sensing subcarriers, respectively. To enhance the performance of sensing, the signals over the sensing subcarriers are optimized adaptively to the data-dependent communication signals, for minimizing the sidelobes of ranging and Doppler estimations. Meanwhile, the

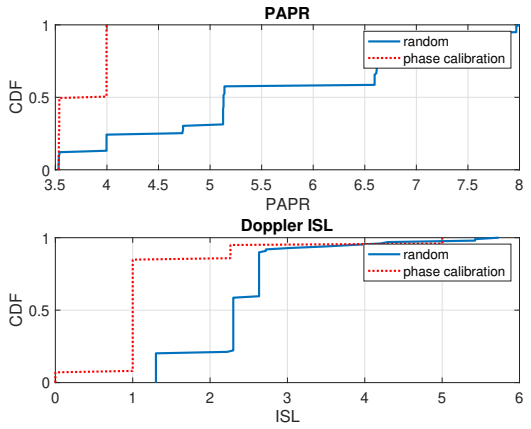

Fig. 7: Comparison of Doppler ISL between random phase and calibrated phase when $M = 4$.

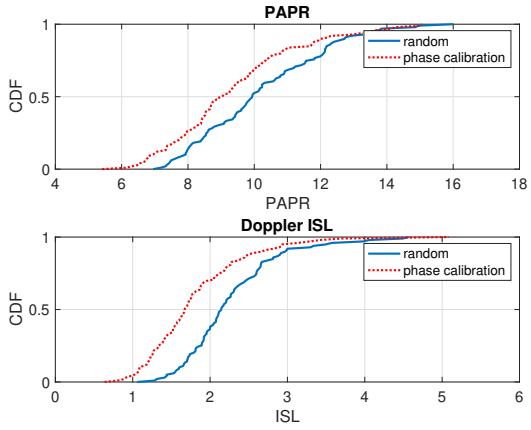

Fig. 8: Comparison of Doppler ISL between random phase and calibrated phase when $M = 64$.

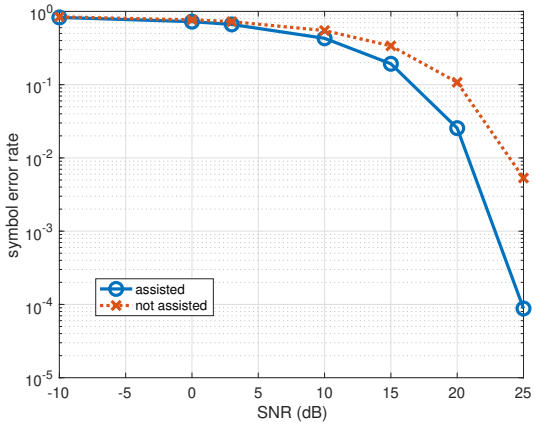

Fig. 9: Symbol error rate with and without sensing subcarrier assistance.

sensing signals determined by the communication signal add redundancies to the data communications, thus improving the capabilities of error detection and correction. The proposed algorithms have been demonstrated using numerical results.

REFERENCES

[1] C. Sturm and W. Wiesbeck, "Waveform design and signal processing aspects for fusion of wireless communications and radar sensing," *Proc. IEEE*, vol. 99, no. 7, pp. 1236–1259, 2011.

[2] B. Paul, A. R. Chiriyath, and D. W. Bliss, "Survey of rf communications and sensing convergence research," *IEEE Access*, vol. 5, pp. 252–270, 2016.

[3] L. Zheng, M. Lops, Y. C. Eldar, and X. Wang, "Radar and communication co-existence: an overview," *arXiv preprint arXiv:1902.08676*, 2019.

[4] F. Liu, C. Masouros, A. Petropulu, H. Griffiths, and L. Hanzo, "Joint radar and communication design: Applications, state-of-the-art, and the road ahead," *IEEE Transactions on Communications*, 2020.

[5] D. Ma, N. Shlezinger, T. Huang, Y. Liu, and Y. C. Eldar, "Joint radar-communications strategies for autonomous vehicles," *IEEE Signal Processing Magazine*, vol. 37, no. 4, pp. 85–97, 2020.

[6] L. Han and K. Wu, "Joint wireless communication and radar sensing systems–state of the art and future prospects," *IET Microwaves, Antennas & Propagation*, vol. 7, no. 11, pp. 876–885, 2013.

[7] A. R. Chiriyath, B. Paul, G. M. Jacyna, and D. W. Bliss, "Inner bounds on performance of radar and communications co-existence," *IEEE Transactions on Signal Processing*, vol. 64, no. 2, pp. 464–474, 2015.

[8] A. R. Chiriyath, B. Paul, and D. W. Bliss, "Radar-communications convergence: Coexistence, cooperation, and co-design," *IEEE Transactions on Cognitive Communications and Networking*, vol. 3, no. 1, pp. 1–12, 2017.

[9] W. Zhang, S. Vedantam, and U. Mitra, "Joint transmission and state estimation: A constrained channel coding approach," *IEEE Transactions on Information Theory*, vol. 57, no. 10, pp. 7084–7095, 2011.

[10] J. R. Guerci, R. M. Guerci, A. Lackpour, and D. Moskowitz, "Joint design and operation of shared spectrum access for radar and communications," in *IEEE Radar Conference*. IEEE, 2015, pp. 761–766.

[11] A. D. Harper, J. T. Reed, J. L. Odom, and A. D. Lanterman, "Performance of a joint radar-communication system in doubly-selective channels," in *49th Asilomar Conference on Signals, Systems and Computers*. IEEE, 2015, pp. 1369–1373.

[12] G. Jacyna, B. Fell, and D. McLemore, "A high-level overview of fundamental limits studies for the darpa ssparc program," in *IEEE Radar Conference*. IEEE, 2016, pp. 1–6.

[13] B. Reynders and S. Pollin, "Chirp spread spectrum as a modulation technique for long range communication," in *2016 Symposium on Communications and Vehicular Technologies (SCVT)*. IEEE, 2016, pp. 1–5.

[14] D. Kellett, D. Garmatyuk, Y. J. Morton, and S. Mudaliar, "Radar communications via random sequence encoding," in *2017 18th International Radar Symposium (IRS)*. IEEE, 2017, pp. 1–9.

[15] S. H. Dokhanchi, B. S. Mysore, K. V. Mishra, and B. Ottersten, "A mmwave automotive joint radar-communications system," *IEEE Transactions on Aerospace and Electronic Systems*, vol. 55, no. 3, pp. 1241–1260, 2019.

[16] S. Dwivedi, M. Zoli, A. N. Barreto, P. Sen, and G. Fettweis, "Secure joint communications and sensing using chirp modulation," in *2020 2nd 6G Wireless Summit (6G SUMMIT)*. IEEE, 2020, pp. 1–5.

[17] N. Levanon, *Radar Signals*. Wiley-IEEE Press, 2004.

[18] H. He, J. Li, and P. Stoica, *Waveform Design for Active Sensing Systems: A Computational Approach*. Cambridge University Press, 2012.

[19] S. Litsyn, *Peak Power Control in Multicarrier Communications*. Cambridge University Press, 2004.

[20] R. O'Neill and L. B. Lopes, "Performance of amplitude limited multitone signals," in *IEEE Vehicular Technology Conference (VTC)*. IEEE, 1994.

[21] M. Sharif and B. Hassibi, "A deterministic algorithm that achieves the pmepr of c log n for multicarrier signals," in *IEEE International Conference on Acoustic, Speech and Signal Processing (ICASSP)*. IEEE, 2003.

[22] J. Tellado and J. M. Cioffi, "Peak power reduction for multicarrier transmission," in *IEEE Global Communications Conference (Globecom)*. IEEE, 1998.